Fault Detection for PMSM Motor Drive Systems by Monitoring Inverter Input Currents

Jing Li[1], Mark Sumner[2], He Zhang[1, 2], Jesus Arellano-Padilla[2],*

[1] Department of Electrical and Electronic Engineering, University of Nottingham, Ningbo, China,315100

[2] Department of Electrical and Electronic Engineering, University of Nottingham UK, NG7 2RD

Abstract —

This paper has proposed a fault detecting method for DC supplied permanent magnet synchronize motor (PMSM) drive systems by monitoring the drive DC input current. This method is based on the fault signal propagation from the torque disturbance on the motor shaft to the inverter input currents. The accuracy of this fault signal propagation is verified by the Matlab simulation and experiment tests with the emulated faulty conditions. The feasible of this approach is shown by the experimental test conducted by the Spectra test rig with the real gearbox fault. This detection scheme is also suitable for monitoring other drive components such as the power converter or the motor itself using only one set of current transducers mounted at the DC input side.

***Index Terms*: Faulty condition, Fault Detection, Motor Drive System, Fault Signal Propagation, PWM inverter**

Nomenclature

f_r	motor rotation frequency
f_f	fault(disturbance) frequency
f_e	motor excitation frequency
T_d	Torque disturbance applied on the motor
T_{df} , φ_f	the amplitude and phase of the torque disturbance caused by faults
i_{qf}	*disturbance* current in the torque producing current
I_{qf}, φ_i	amplitude and phase of i_{qf}
w_{rf}, φ_w	amplitude and phase of the speed disturbance caused by the torque disturbance
i_{dcf}	Inverter DC side disturbance current
I_{DC}	DC component of the inverter DC side current
u_{dc}	Inverter DC side voltage
J,B	motor inertia and friction
L_d,L_q	motor d,q axix inductance
P	number of pole pairs
R_s	motor stator resistance
Kt	motor torque constant

1. INTRODUCTION

To detect faults, lots of methods have been studied and implemented to enhance the reliability and stability of the motor drive systems. The condition monitoring of the motor drive systems can be achieved by the vibration monitoring [1, 2], the flux measurement [3], and the thermal monitoring [4]. Benefited from the high power density and high efficiency, PMSMs have been generally employed in "more electric aircraft" (MEA) [5] and also in many applications such as power steering in automobiles. For these applications it is usually not feasible to use the additional complexity of vibration or thermal measurements [6] due to cost, space or reliability concerns.

*Corresponding author, Tel.:+86(574)88180000-8234;
Email address: He.Zhang@nottingham.edu.cn

Motor current signature analysis(MCSA) [7] is the most widely applied approach to detect faults of motor drive systems, especially for mechanical faults [8]. MCSA measures and processes the stator currents, and then detect changes in the harmonic contents to indicate any abnormality in the machines. However, measurement of the machine currents may be impractical in some cases such as those where the power converter and the machine are integrated in a single unit or when the access to the machine and the power converter is impractical due to their location [9, 10]. The use of integrated drives is being encouraged in aerospace and automotive applications; if there is a fault it is easier to replace the full unit without affecting other systems. Integrated drives are usually considered as a 'black box' purchased from a third party so the access to internal signals is not always possible. An alternative approach to MCSA is therefore to monitor the input currents to the motor drive system itself rather than the winding currents of the machine, as these measurements can be made externally and independently of any drive controller, and will also show evidence of drive faults.

This may be achieved by monitoring the drive's supply currents. In [9], the author proposed a new approach to detect the turn-to-turn short circuit fault of the generators by using only the dc current information because of the difficulty to access the built-in rectifier ac current or the voltage of the generator.

Electrical power systems have developed significantly in aircraft and ships over recent decades [11]. Aircraft electric power systems evolved from 28V DC system in 1940s and 1950s to recent 28V/270 V DC and 115V/230V AC systems [12]. The US Air force and the US Navy have placed a large emphasis on developing a 270V DC system [11]. The use of higher voltages has improved efficiency of power generation and weight savings. The typical future power system layout for the MEA applications is shown in Fig1. It can be seen the DC bus plays an essential role in the whole power systems. However the increasing application of electrical equipment in DC and AC power systems in aircraft and marine power systems makes it essential to detect the onset of fault conditions in the system at an early stage.

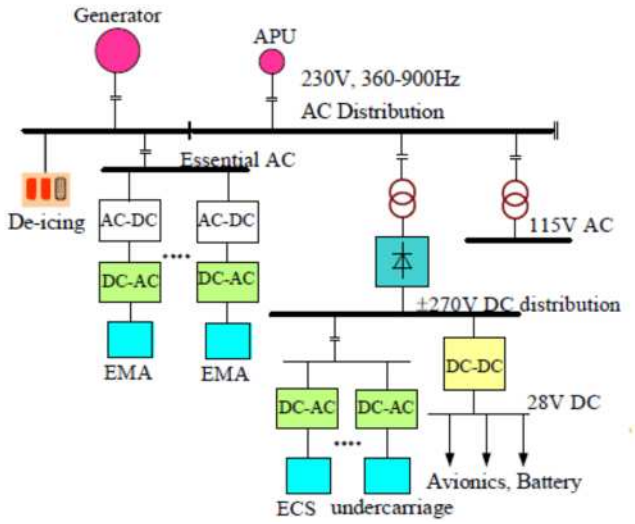

Fig1. The future power electrical systems for MEA

This paper proposed a fault detection approach by sensing the DC supply current which is based on quantitative analyses of the propagation path that a fault propagates through the drive from the torque disturbance to the DC input current of a DC supplied PMSM drive system. This fault signal propagation includes the effect of the PMSM (through its torque producing current i_q and the speed ripple) and the PWM inverter. The analysis predicts the magnitude of the harmonics in the inverter input current caused by the torque disturbances of the motor shaft. These quantitative analyses are very important since the proposed approach could be used to predict the impact of faults on the DC bus and also may help to determine the detection limitation of the fault detection approach. This research pays more attention to mechanical faults; however, this approach is also feasible to detect the faults at the power converters and motor electrical faults.

2. FAULTS IN SERVO DRIVE SYSTEMS

Majority of mechanical faults and electrical faults of a motor drive system generate torque disturbances at the motor shaft. Bearing faults and gearbox faults are most common mechanical faults of electrical machines. Each kind of fault has a series of characteristic disturbance frequencies related to it. To detect and diagnose a specific fault by sensing disturbance harmonic contents of the supply current caused by torque disturbances, the machine's speed and the characteristic frequencies of specific faults need to be known.

2.1 Bearing Faults

Bearing fault detection is essential and indispensable, since 40%-50% of all motor faults result from bearing failure [13] Bearing faults can be classified as outer race defects, inner race defects, ball defects and cage defects. All these faults generate an increment in vibration and therefore a torque disturbance associated with the fault [10]. The vibration frequency will be determined by the motor speed, the bearing fault type and the bearing geometry. Typical disturbance frequencies are given in many documents such as [14].

*Corresponding author, Tel.:+86(574)88180000-8234;
Email address: He.Zhang@nottingham.edu.cn

2.2 Gearbox Faults

When defective gears are present, a vibration will be generated and the spectrum of the vibration can therefore be measured and identify the gear fault. For a single defect on a single tooth such as a cracked, broken, or missing tooth, a shock pulse will be caused each time this defect tooth meshes [15]. Therefore, the vibrations will be $n \cdot f_r$ and also will show up as the sideband of the mesh frequencies: $n \cdot f_m \pm f_r$ where n= 1,2,3,… and f_m is the gear mesh frequency ($f_m = N \cdot f_r$, where N is teeth number of the gear [6]). As the sidebands of the mesh frequencies are high, they are normally measured using an accelerometer. If there are two defective teeth, two shock pulses will be created in each revolution and the time interval between these two shock pulses is proportional to the angle between the two defective teeth [15].

The author only considered the faults that appear as a torque disturbance on the machine shaft in this work, and does not consider additional flux coupling effects due to non-uniform airgap.

3 FAULT PROPAGATION THROUGH THE DRIVE SYSTEM

The fault signal propagation through the torque disturbance at the motor shaft to the inverter input current will be briefly given in this section. The conventional layout of a DC supplied three phase motor drive system is illustrated in Fig.2. The torque disturbance generated by the faulty condition will be transferred into the Iq current and the rotor speed with frequency shift, then further be seen at the inverter input currents as the disturbance harmonic content. Finally, the presence of unexpected fault spectra or significantly changed harmonics in the supply input currents provides the clue to detect the fault.

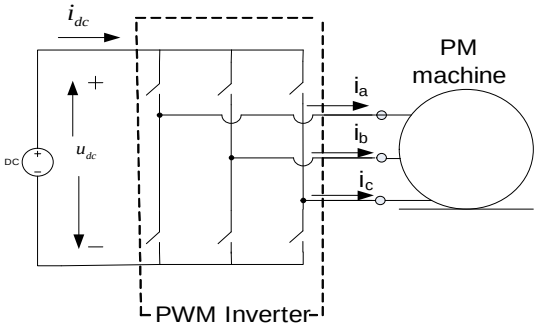

Fig. 2. DC Supplied PMSM motor drive system

To simplify the analysis, the disturbance signal propagation through the drive system is split into two parts: the disturbance torque transfer function through the vector controlled PMSM machine and the disturbance signal propagation through PWM inverter. Assuming a fault occurring at the motor shaft while PMSM is operating in steady state causes torque disturbances at f_f which is determined by the fault type as described in the previous section. For the first part, the transfer function from the torque disturbance to *Iq* current is given in (1) [16]. The disturbance frequency in i_q is f_f and disturbances in motor

winding currents are two sideband harmonic content: $|f_e \pm f_f|$ around the PMSM fundamental frequency f_e. [17-19]

$$G_{I_q 2T_d}(s) = \frac{I_q(s)}{T_d(s)} = \frac{-\frac{1}{Js+B}\cdot G_{sc}(s)\cdot G_{clc}(s)}{1+G_{sc}(s)G_{clc}(s)\frac{1}{Js+B}K_t} \quad (1)$$

where $G_{sc}(s)$ is the speed controller; K_t is the machine's torque constant, J is the inertia and B is the frictional coefficient given in the Appendix. $G_{clc}(s)$ is the transfer function of the closed loop current control which is given by[19]:

$$G_{clc}(s) = \frac{I_q(s)}{I_q^*(s)} = [G_{cc}(s)\frac{1}{L_q s + R_s}]/[1+G_{cc}(s)\frac{1}{L_q s+R_s}] \quad (2)$$

where $G_{cc}(s)$ is the current controller, L_q the q-axis inductance, and R_s the stator resistance. Both speed and current controllers are tuned by the root locus method. The amplitude and phase of i_{qf} can be derived as:[19]

$$I_{qf} = \left|G_{I_q 2T_d}(s)\right|_{s=j\varpi_f}\cdot T_{df}\ ,\quad \varphi_i = \angle G_{I_q 2T_d}(s)\Big|_{s=j\varpi_f} + \varphi_f \quad (3)$$

where T_{df} and φ_f are the amplitude and phase of the torque disturbance at the fault frequency f_f caused by the specific fault. In a similar way, the speed fluctuation caused by the fault can be calculated by using expression (4), which relates the motor speed to the torque disturbance:

$$G_{\varpi_r 2T_d}(s) = \frac{\varpi_r(s)}{T_d(s)} = 1/(Js+B)[1+G_{cs}(s)G_{clc}(s)\frac{1}{Js+B}K_t] \quad (4)$$

The speed change in terms of amplitude and phase response (ϖ_{rf} and ϕ_{ϖ}) due to a torque disturbance can be expressed as:

$$\varpi_{rf} = \left|G_{\varpi 2T_d}(s)\right|_{s=j\varpi_f}\cdot T_{df}\ ,\quad \varphi_{\varpi} = \angle G_{\varpi 2T_d}(s)\Big|_{s=j\varpi_f} + \varphi_f \quad (5)$$

Assuming no conduction loss in the PWM inverter, the instantaneous active power conservation is applied to derive the disturbance signal propagation through the PWM inverter. The disturbance current in inverter input current is given in (6).[19]

$$i_{idcf}(t) = \frac{3}{2U_{dc}}\sqrt{a^2+b^2+2ab\cos(\varphi_1+\varphi_i-\varphi_{\varpi})}\sin(\varpi_f t+\varphi_2) \quad (6)$$

where $\varphi_i, \varphi_{\varpi}$ are defined in (3) and (5) respectively, and Iq is the DC component of iq. U_{dc} is the mean voltage of inverter (DC side). λ is the flux generated by the rotor.

$$a = I_{qf}\sqrt{(2R_s I_q + P\cdot\varpi_r^*\cdot\lambda)^2 + (L_q I_q \varpi_f)^2}$$

$$b = I_q\lambda\cdot P\cdot\varpi_{rf}\ ,\quad \varphi_1 = \tan^{-1}(L_q I_q\varpi_f / (2R_s I_q + P\cdot\varpi_r^*\cdot\lambda))\ ,$$

$$\varphi_2 = \tan^{-1}\left(\frac{a\cdot\sin(\varphi_i+\varphi_1)+b\cdot\sin(\varphi_{\varpi})}{a\cdot\cos(\varphi_i+\varphi_1)+b\cdot\cos(\varphi_{\varpi})}\right)$$

*Corresponding author, Tel.:+86(574)88180000-8234;
Email address: He.Zhang@nottingham.edu.cn

4 Simulation Studies

To verify the accuracy of this disturbance signal propagation through DC supplied motor drive systems given in Fig.1, Matlab and Plecs time-domain simulations were conducted. To match the experimental test rig, all the real electrical and mechanical parameters from the test rig given in Table A in appendix were adopted for the simulation study. All the power switches and component are simulated at ideal conditions except 0.7v forward voltage drop and on-resistance of diodes. Similar to the real operation condition, the PMSM is operating at $f_r = 20Hz$ with 90% of the rated load. To have a good diversity, a series of torque disturbance frequencies including 12Hz, 22Hz, 45Hz, 55Hz, 65Hz, 72Hz and 82Hz were applied with amplitude as 2Nm, which is 16% of the rated torque. The disturbance current in I_q caused by the torque disturbance has been calculated with (2) and compared with simulation results as shown in Fig.3. The error is less than 0.01%. Two different speed loop bandwidths (2.2Hz and 5Hz) have been used. From Fig.3, it is obvious that a higher bandwidth controller provides a stronger propagation of the disturbance to the motor current. From Fig.3, it can be seen that the i_q disturbance current (i_{qf}) reduces as the disturbance frequency increases over the disturbance frequency range.

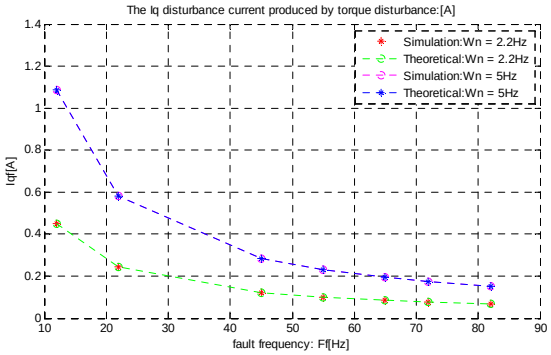

Fig.3 Simulation and theoretical results for the I_q disturbance current with different speed loop bandwidth

The theoretical results for the inverter input side disturbance current (i_{dcf}) calculated with (6) are compared with the simulation results and shown in Fig.4. The error for the inverter input side disturbance current is less than 0.1%.

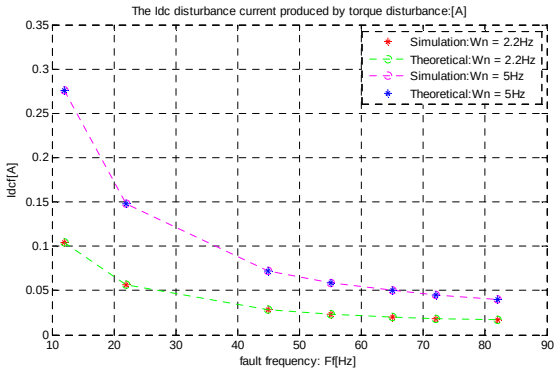

Fig.4 Comparison between Simulation and theoretical results for the disturbance current in the inverter input side current

5 Experimental Results with Emulated Faulty Condition

To verify the accuracy of the fault signal propagation given in previous section, an experiment rig including a 6-pole 3.82kW PM industrial machine, a DC machine working as load, Chroma DC power supply and DSP and FPGA control platform, was set up. Machine and circuit parameters are shown in the Table A in Appendix. The speed loop controller is designed as $G_{cs}(s) = (0.47s + 5.1)/s$ to give the bandwidth of the speed loop as 2.2Hz and the current loop controller is employed $G_{cc}(s) = (21s + 30660)/s$ to give the nature frequency of the current loop as 433 Hz. A three-phase PWM inverter is implemented with 10kHz switching frequency. The sampling frequency of the speed loop and the current loop are 200 Hz and 10kHz respectively. A bespoke DSP and FPGA control platform has been set up to fulfil the vector control of the PMSM. A DC dynamometer is used to emulate specific faults by imposing controlled sinusoidal torque disturbances at different frequencies. This torque disturbance frequency was varied as 12Hz, 22Hz, 45Hz, 55Hz, 65Hz, 72Hz and 82Hz.

The motor was operated under approximately 90% of the rated load while the torque disturbance amplitude was set as 4Nm. The inverter input current was measured by an oscilloscope and processed by MATLAB Fast Fourier Transform (FFT) program [20] to extract the disturbance harmonic contents which are shown in Fig.5 and compared with theoretical results calculated by (6). From Fig. 6, a good agreement has been achieved where the maximum error is about 8%. The error may be caused by non-linearities which have been neglected in the theoretical analysis. From the simple experimental tests considered here it can be seen that torque disturbance frequencies in the range 0-100Hz can be detected by analyzing the inverter input current.

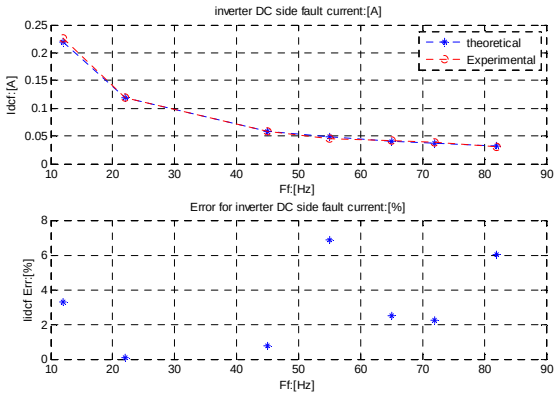

Fig. 5 Inverter DC side disturbance currents and errors between theoretical and experimental results

6 Experimental Results with Gearbox Fault

To investigate the real fault condition, a real gearbox fault has been studied and tested. A second experimental rig called SpectraQuest Rig [21] has been built up which comprises the same PMSM motor, a programmable magnetic brake and a 2 stage external spur gearbox shown in Fig.6 and the torque transducer installed on the motor shaft. The gear ratio of the first stage of gear is 32/80=0.4 and the gear ratio of the second stage of gear is 48/64 = 0.75. A gearbox fault was introduced by removing a tooth from the gear on the input shaft given in Fig 7.

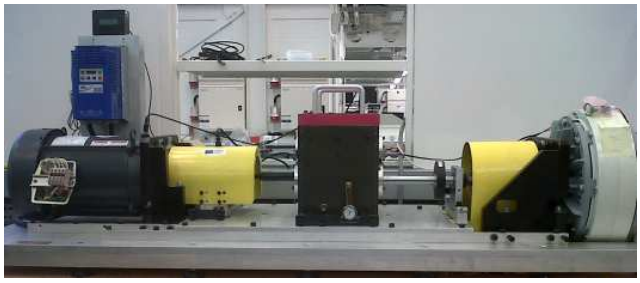

Fig. 6 Spectra Rig layout

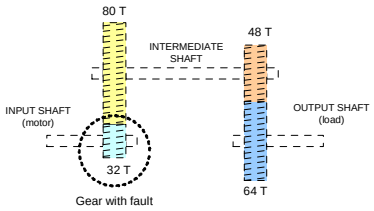

Fig. 7 two stage gearbox with a missing tooth on the input shaft

The load torques with both healthy and faulty gearbox are measured by the torque transducer and illustrated and compared in Fig. 8, when the motor was operating at 20Hz with the full load. The resultant torque disturbance appeared at the motor rotation frequency (f_r =20 Hz), $2f_r$, $4f_r$ and the rotation shaft frequency for the intermediate shaft ($f_{r1} = 0.4*20 = 8Hz$). The inverter DC supply current spectrum under the healthy and faulty conditions are also measured, analyzed with FFT calculation and compared in Fig. 8. Comparing to the disturbances at load torque (T_d) and inverter DC current (I_{dc}) under healthy conditions as shown in Fig. 8, the faulty gearbox gives a more significant torque disturbance and DC current disturbance at $2f_r$ (40Hz). This inverter DC supply current disturbance therefore can be used as an indication of the faulty condition.

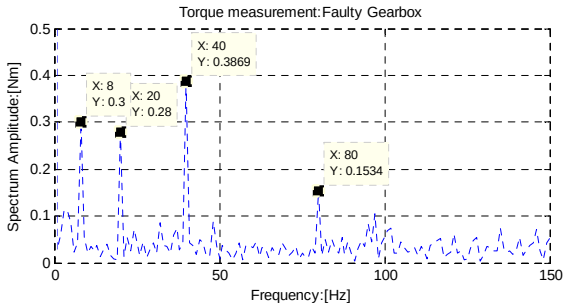

Fig 8.a) Load torque spectrum with faulty gearbox

*Corresponding author, Tel.:+86(574)88180000-8234;
Email address: He.Zhang@nottingham.edu.cn

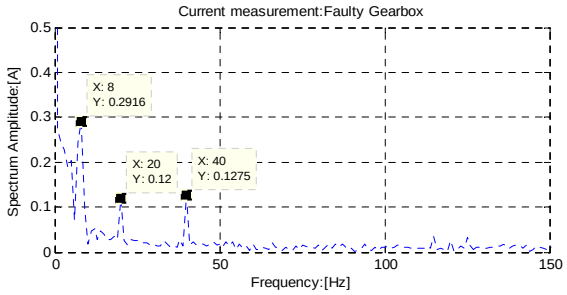

Fig 8.b) Inverter DC supply current spectrum with faulty gearbox

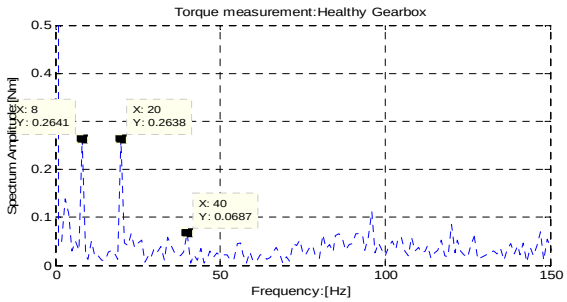

Fig 9.c) Load torque spectrum with healthy gearbox

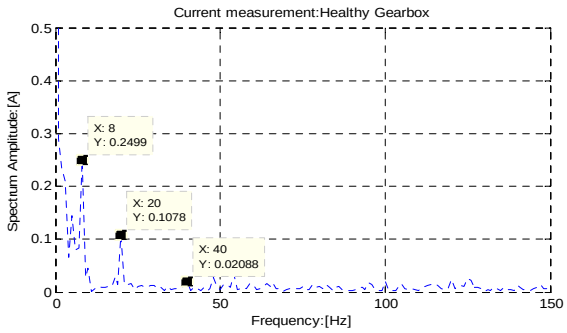

Fig 8.d) Inverter DC supply current spectrum with healthy gearbox

7 CONCLUSIONS

This paper has proposed a fault detecting method for DC supplied PMSM motor drive system by monitoring the input currents. This method is based on the fault signal propagation through the torque disturbance on the motor shaft to the inverter input currents. The accuracy of this fault signal propagation is verified the Matlab simulation study and experiment tests with the emulated faulty conditions. The feasible of this approach is shown by the experimental test conducted by the Spectra test rig with the gearbox fault. This scheme is also suitable for monitoring other drive components such as the power converter or the motor itself using only one set of current transducers mounted at the DC input side, and this is part of on-going research.

ACKNOWLEDGEMENTS

This work is supported by the Ningbo Science and Technology Bureau, China under Grant 2014A35007 and 2013A31012.

Appendix

TABLE A: ELECTRICAL PARAMETERS FOR THE PM MACHINE

Number of pole pair:	3
Rated speed:	3000 (rpm)
Rated torque:	12.2 (Nm)
Rated power:	3.82 (kW)
Kt:	1.6 (Nm/A)
Ke:	98 (Vrms/krpm)
Inertia:	20.5 (kgcm^2)
R (ph-ph):	0.94
L (ph-ph):	8.3mH

*Corresponding author, Tel.:+86(574)88180000-8234;
Email address: He.Zhang@nottingham.edu.cn

References

[1] V. Climente-Alarcon, J. A. Antonino-Daviu, F. Vedre, x00F, S. o, and R. Puche-Panadero, "Vibration Transient Detection of Broken Rotor Bars by PSH Sidebands," *IEEE Transactions on Industry Applications*, vol. 49, no. 6, pp. 2576-2582, 2013.

[2] O. O. Ogidi, P. S. Barendse, and M. A. Khan, "Detection of Static Eccentricities in Axial-Flux Permanent-Magnet Machines With Concentrated Windings Using Vibration Analysis," *IEEE Transactions on Industry Applications*, vol. 51, no. 6, pp. 4425-4434, 2015.

[3] L. Frosini, C. Harli, x015F, ca, L. Szab, and x00F, "Induction Machine Bearing Fault Detection by Means of Statistical Processing of the Stray Flux Measurement," *IEEE Transactions on Industrial Electronics*, vol. 62, no. 3, pp. 1846-1854, 2015.

[4] J. Hey, A. C. Malloy, R. Martinez-Botas, and M. Lamperth, "On-line monitoring of electromagnetic losses in an electric motor indirectly through temperature measurement," *IEEE Transactions on Energy Conversion*, vol. PP, no. 99, pp. 1-1, 2016.

[5] A. M. El-Refaie, "Fault-tolerant permanent magnet machines: a review," *IET Electric Power Applications*, vol. 5, no. 1, pp. 59-74, 2011.

[6] L. R. Peter Tavner, Jim Penman,Howard Sedding, *Condition Monitoring of Rotating Electrical Machines* (Power and Energy Series 56). London: The Institution of Eingineering and Technology,London,UK, 2008.

[7] S. B. Lee *et al.*, "Identification of False Rotor Fault Indications Produced by Online MCSA for Medium-Voltage Induction Machines," *IEEE Transactions on Industry Applications*, vol. 52, no. 1, pp. 729-739, 2016.

[8] J. A. Corral-Hernandez *et al.*, "Transient-Based Rotor Cage Assessment in Induction Motors Operating With Soft Starters," *IEEE Transactions on Industry Applications*, vol. 51, no. 5, pp. 3734-3742, 2015.

[9] S. Cheng and T. G. Habetler, "Using Only the DC Current Information to Detect Stator Turn Faults in Automotive Claw-Pole Generators," *IEEE Transactions on Industrial Electronics*, vol. 60, no. 8, pp. 3462-3471, 2013.

[10] J. Arellano-Padilla, M. Sumner, C. Gerada, and J. Li, "A novel approach to gearbox condition monitoring by using drive rectifier input currents," in *Power Electronics and Applications, 2009. EPE '09. 13th European Conference on*, 2009, pp. 1-10.

[11] A. S. Ian Moir, *aircraft systems*, Third Edition ed. (Ian Moir, Allan Seabridge and Roy Langton). West Sussex: John Wiley&Sons Ltd, 2008.

[12] *AIRCRAFT ELECTRIC POWER CHARACTERISTICS*, 2004.

[13] S. Nandi, H. A. Toliyat, and L. Xiaodong, "Condition monitoring and fault diagnosis of electrical motors-a review," *Energy Conversion, IEEE Transactions on*, vol. 20, no. 4, pp. 719-729, 2005.

[14] G. Xiang and Q. Wei, "Bearing Fault Diagnosis for Direct-Drive Wind Turbines via Current-Demodulated Signals," *Industrial Electronics, IEEE Transactions on*, vol. 60, no. 8, pp. 3419-3428, 2013.

[15] V. Wowk., *Machinery vibration : measurement and analysis*. 1991.

[16] J. Li, M. Sumner, J. Arellano-Padilla, and H. Zhang, "Fault Signal Propagation through the PMSM Motor Drive System," *IEEE Transactions on Industry Applications*, vol. PP, no. 99, pp. 1-1, 2017.

[17] P. Zhang, T. G. Habetler, Y. Du, and B. Lu, "A Survey of Condition Monitoring and Protection Methods for Medium-

Voltage Induction Motors," *Industry Applications, IEEE Transactions on*, vol. 47, no. 1, pp. 34-46, 2011.

[18] M. S. Odavic, M.; Wheeler, P. ;J, Li, "Real-time fault diagnostics for a permanent magnet synchronous motor drive for aerospace applications," in *Energy Conversion Congress and Exposition (ECCE), 2010 IEEE*, 2010, pp. 3044-3049.

[19] J. Li, M. Sumner, J. Arellano-Padilla, and G. Asher, "Condition monitoring for mechanical faults in motor drive systems using the recifier input currents," in *Power Electronics, Machines and Drives (PEMD 2010), 5th IET International Conference on*, 2010, pp. 1-6.

[20] V. K. Madisetti, *The digital signal processing handbook. Digital signal processing fundamentals*, 2nd ed ed. (Electrical engineering handbook series). London Boca Raton.Fla.;London:CRC Press, c2010., 2010.

[21] *Manual of Drivetrain Diagnostics Simulator by SpectraQuest,Inc.* 2010.

*Corresponding author, Tel.:+86(574)88180000-8234;
Email address: He.Zhang@nottingham.edu.cn